On the decline of 1st and 2nd order sensitivity with eccentricity

Robert F. Hess
McGill Vision Research, Department of Ophthalmology, McGill University, Montréal, Québec, Canada

Daniel H. Baker
School of Life & Health Sciences, Aston University, Birmingham, UK

Keith A. May
Vision Science Research Group, School of Life Sciences, University of Bradford, Bradford, UK

Jian Wang
McGill Vision Research, Department of Ophthalmology, McGill University, Montréal, Québec, Canada

We studied the relationship between the decline in sensitivity that occurs with eccentricity for stimuli of different spatial scale defined by either luminance (LM) or contrast (CM) modulation. We show that the detectability of CM stimuli declines with eccentricity in a spatial frequency-dependent manner, and that the rate of sensitivity decline for CM stimuli is roughly that expected from their 1st order carriers, except, possibly, at finer scales. Using an equivalent noise paradigm, we investigated the possible reasons for why the foveal sensitivity for detecting LM and CM stimuli differs as well as the reason why the detectability of 1st order stimuli declines with eccentricity. We show the former can be modeled by an increase in internal noise whereas the latter involves both an increase in internal noise and a loss of efficiency. To encompass both the threshold and suprathreshold transfer properties of peripheral vision, we propose a model in terms of the contrast gain of the underlying mechanisms.

Keywords: periphery, first order, second order, internal equivalent noise, contrast gain control

Citation: Hess, R. F., Baker, D. H., May, K. A., & Wang, J. (2008). On the decline of 1st and 2nd order sensitivity with eccentricity. *Journal of Vision, 8*(1):19, 1–12, http://journalofvision.org/8/1/19/, doi:10.1167/8.1.19.

Introduction

Visual information is not solely restricted to variations in luminance across the image (1st order variations); variations in contrast (2nd order variations) also play an important role in defining features (Johnson & Baker, 2004). Not unexpectedly, cells in the visual cortex are tuned for both 1st and 2nd order image features (Zhou & Baker, 1993). Even though some cells in early visual areas perform both 1st and 2nd order processing, the neural circuits underlying these two processes are very different (Baker, 1999). In particular, 2nd order processing involves an initial stage of linear filtering (similar to its 1st order counterpart), but following a nonlinearity such as rectification, the signal is subjected to a second stage of linear filtering at a lower scale than that of the first stage (i.e., filter–rectify–filter or FRF model).

It has recently been shown that the 2nd order system, like its 1st order counterpart, is composed of mechanisms that are tuned for spatial frequency and orientation (Ellemberg, Allen, & Hess, 2006). However, the overall envelope of sensitivity of all second order tuned detectors is about an order of magnitude lower than that of its 1st order counterpart (Hutchinson & Ledgeway, 2006; Sutter, Sperling, & Chubb, 1995).

One of the characteristic features of mammalian visual processing is its strong dependence on visual field eccentricity (Wertheim, 1894). The visual system allocates more resources to central vision; in the retina there is a greater density of most cells subserving central vision (Rodieck, 1973), and in the cortex, more cortical area is devoted to the central part of the visual field (Daniel & Whitteridge, 1961). Furthermore, in the retina, the receptive field size of retinal ganglion cells increases with eccentricity (Peichl & Wassle, 1979) and in the cortex, the mean receptive field size is larger in peripheral vision (Hubel & Wiesel, 1977).

In terms of psychophysics, sensitivity to a 1st order, luminance-defined stimulus of any given size falls off as a function of eccentricity (Robson & Graham, 1981); the higher its spatial frequency, the greater the falloff in

doi: 10.1167/8.1.19 Received May 23, 2007; published January 28, 2008 ISSN 1534-7362

sensitivity with eccentricity (in degrees of visual angle). This would suggest that not only does the average receptive field size change with eccentricity, reflecting a loss of smaller receptive fields, but also sensitivity of cells of a particular receptive field size also decline with eccentricity.

There are at least 3 different types of falloff with eccentricity for 1st order spatial targets (Pointer & Hess, 1989) when eccentricity is considered in terms of units relative to the size of a spatial target (i.e., eccentricity in units of spatial periods); stimuli whose spatial frequency is above 1 cpd exhibit one rule, those between 0.2 and 1 cpd exhibit another rule, and those below 0.2 cpd exhibit yet another rule. These different characteristic sensitivity falloffs for different spatial stimuli may reflect their different processing sites within the cortex. Although much is known about this strong eccentricity dependence, much less is known about why sensitivity at any one particular spatial frequency falls off.

In this study, we address three questions that bear upon the above issues:

1. "Does the sensitivity for detecting a 2nd order stimulus falloff at the same rate as 1st order stimuli of the same spatial frequency?"
2. "Why is there a loss of sensitivity for 1st order stimuli with eccentricity?"
3. "Why is the fovea less sensitive for detecting 2nd order stimuli compared with their 1st order counterparts?"

In terms of the first question, there is an obvious prediction. Since the rate sensitivity declines with eccentricity (in degrees) depends directly on the spatial frequency of 1st order stimuli (Robson & Graham, 1981), and 2nd order processing comprises an initial stage of higher frequency 1st order processing, one might expect a more rapid falloff for 2nd order stimuli whose modulation frequency matched that of a 1st order stimulus. This, however, need not be the case since the foveal sensitivity for detecting 2nd order stimuli is much less than that of comparable 1st order stimuli, allowing the possibility that carrier detection is not the dominant influence.

In terms of the second question, namely the reason for the loss of sensitivity with eccentricity for 1st order stimuli, there are a number of possibilities. One is that the peripheral population of cells are less efficient at processing information compared with their centrally located counterpart, possibly because there are fewer of them (Rodieck, 1973). Alternatively, peripherally located cells could be individually more noisy than their central counterparts as a consequence of their rod input which, while not contributing signal, may contribute noise.

Finally, 2nd order stimuli may be harder to detect than their 1st order counterparts for number of reasons. First, their higher spatial frequency first stage may be either more noisy (Pelli, 1990) or more quantum-limited (Banks, Geisler, & Bennett, 1987; Van Nes & Bouman, 1967) and therefore less efficient. Secondly, the loss in sensitivity may have nothing to do with first stage processing but involve less efficient pooling of population responses.

To address these questions we undertake two separate series of experiments. In Part I, we address the question concerning the relative falloff in sensitivity with eccentricity for 1st and 2nd order stimuli of the same spatial periodicity. In Part II, using an equivalent noise approach we address two issues; the 1st order falloff in sensitivity with eccentricity and the reduced sensitivity of foveal 2nd order stimuli.

Methods

Apparatus and stimuli

Stimuli were displayed using either a Bits++ box (Part I) or a VSG 2/5 (Part II), both supplied by Cambridge Research Systems (Kent, UK). In Part I, the monitor was a Sony CPD-520 GS (mean luminance 50 cd/m^2), running at 85 Hz. In Part II, a Clinton Monoray monitor (mean luminance 200 cd/m^2) running at 120 Hz was used. Monitors were gamma corrected using standard techniques to compensate for the inherent nonlinearities of CRT displays. Experimental software was written in Matlab (The Mathworks, Inc.) and run on a PC.

Test stimuli were either sinusoidal luminance modulations about the mean value (L) or luminance (LM) or contrast (CM) modulations of a carrier. At a viewing distance of 57 cm, the modulation was always at 1 cpd. In Part I, viewing distances of 28 cm and 171 cm were also tested, resulting in modulation spatial frequencies of 0.5 and 3 cpd.

The carrier for LM and CM stimuli was either a plaid composed of two oblique gratings (±45°) at 4 times the modulation frequency (both experiments) or a patch of 2-d binary noise (Part I only). Carriers were counterphase flickered using a square wave temporal envelope at 10.6 Hz (Part I) or 10 Hz (Part II) (differences in temporal frequency were due to different monitor refresh rates).

Test modulation and carrier were combined either additively (LM) or multiplicatively (CM). In Part I, the unmodulated carrier contrast was always 50%, so that it was suprathreshold at the widest range of eccentricities possible. In Part II, the carrier contrast was reduced to 25% because frame interleaving of the test with the noise mask reduced the available contrast range. As viewing was foveal for all LM and CM stimuli in Part II, the carrier was always greatly suprathreshold.

Noise masks in Part II were 1-d samples of "pink" noise, with a power spectrum proportional to $1/f$, where f is spatial frequency. Each noise sample was low-pass filtered to remove all components above 1 cpd. Thus, the mask consisted only of frequencies equal to and lower than the test modulation. Masks were always oriented horizontally and were combined with test stimuli using a frame

interleaving technique. A new noise mask was generated for each trial and was identical in both intervals (the "twin" condition of Watson, Borthwick, & Taylor, 1997). A control experiment confirmed that the noise masks did not affect detection thresholds for the carrier plaid.

All stimuli were displayed in a two-dimensional Gaussian spatial window, with standard deviation (σ) equal to one complete cycle of the modulation (test) signal.

We express contrast throughout in decibels (dB), calculated as $20.\log_{10}(C\%)$, where C% is contrast expressed as a percentage. In the case of luminance-modulated stimuli, this is Michelson contrast, given by

$$100 \times \frac{L_{max} - L_{min}}{L_{max} + L_{min}}, \quad (1)$$

where L is luminance. For noise stimuli, contrast refers to the RMS (root mean square) contrast, which is equivalent to the standard deviation of the noise. High contrast, static examples of these stimuli are shown in Figure 1.

Subjects

In Part I, two subjects were tested, both of whom were inexperienced psychophysical observers. One (DL) was naive to the aims if the experiment, and the other (JW) was an author. In Part II, JW again participated, along with four additional subjects, all of whom were highly experienced psychophysically (2 postgraduates, 2 postdoctoral fellows). All subjects wore their normal optical correction.

Procedure

Subjects were seated in a darkened room, at the appropriate viewing distance (see above). Stimuli were always presented in the centre of the screen; for peripheral viewing conditions, fixation was away from centre by the appropriate displacement and was with the dominant eye (the nondominant eye was occluded). Stimuli were always presented on the nasal side and did not lie in the blind spot. A fixation point was always displayed, either on screen or on an attached strip of card.

In Part I, a single interval orientation judgment task was used, in which subjects indicated whether the test modulation was horizontal or vertical (753 ms presentation). In Part II, a two-interval forced choice (2IFC) detection paradigm was used, in which subjects indicated the interval containing the test modulation (here the modulation was always horizontal). The null interval thus contained both mask and unmodulated carrier, whereas the test interval contained the mask and the modulated carrier (LM or CM). Stimuli were presented for 750 ms with an interstimulus interval of 500 ms. Subjects responded using a two-button mouse and were given auditory feedback to indicate correctness of response.

Part I was blocked by viewing distance (and hence effective spatial frequency), eccentricity, and stimulus type (L/LM/CM, etc.). Part II was blocked by stimulus type and mask contrast. Subjects completed all eccentricities (or mask contrasts) for a given spatial frequency (or stimulus type) before moving on to the next. The order of blocks was randomly determined.

Thresholds were tracked by two interleaved staircases (Cornsweet, 1962; Wetherill & Levitt, 1965), moving in logarithmic (dB) steps of modulation contrast. In Part I, a 2-down, 1-up rule was used, and in Part II, a 3-down, 1-up rule was used. Staircases terminated after 12 reversals. Experiments in Part I were run between one and three times by each subject, and Part II experiments were run three times. The data were then pooled across sessions, and a cumulative Gaussian was used to estimate the threshold at 75% correct, using either the *psignifit* software (http://www.bootstrap-software.org/psignifit/) for Part I or the Probit analysis (Finney, 1971) for Part II.

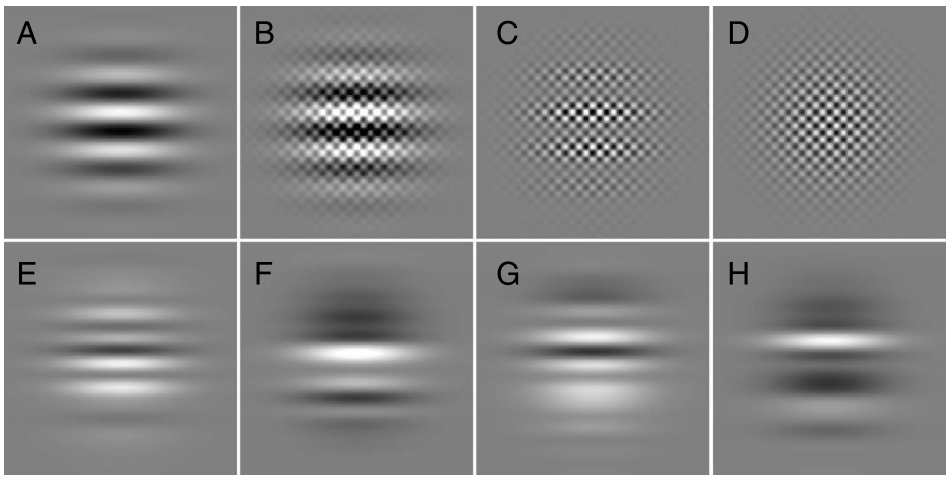

Figure 1. Example stimuli: (A) sinusoidal luminance modulation, (B) luminance modulation of carrier (LM), (C) contrast modulation of carrier (CM), (D) unmodulated carrier, (E–H) example 1-d noise masks.

Modeling

The noisy liner amplifier model (LAM) (Lu & Dosher, 1999; Pelli, 1981) was fit to the data for each experiment in Part II. The model is defined by the equation,

$$\text{resp} = \frac{BC}{\sqrt{N_{\text{ext}}^2 + N_{\text{int}}^2}}, \quad (2)$$

where C is test contrast, N_{ext} is external noise (mask) contrast, B is sensitivity, and N_{int} is an estimate of internal noise level. For each mask contrast (N_{ext} level), the test contrast was systematically varied until the model response exceeded a criterion value, which was set arbitrarily to 0.95 (d' at 75% correct in 2AFC tasks).

Best fitting parameters were determined using a simplex algorithm (Nelder & Mead, 1965). The model was fit using either 3 or 4 free parameters. In the 4-parameter model, separate values of B and N_{int} were permitted for each condition. In the 3-parameter models, one parameter was constrained to take on the same value across both conditions. Using a nested hypothesis F-test, the 3- and 4-parameter fits can be compared statistically to determine whether the change in threshold across conditions is best described by a change in internal noise, or a change in sensitivity (efficiency).

Results

Part I: Eccentricity dependence

In Figure 2, contrast thresholds in decibels (see above) are plotted against stimulus eccentricity for two subjects (JW and DL) for three spatial frequencies; 0.5 (left), 1 (middle), and 3 cpd (right). In each case, a number of stimuli are compared (see Figure 1); simple luminance modulation at frequency f (L), a compound luminance modulation where a frequency f has a fixed 50% contrast $4f$ plaid added to it (LM), contrast modulation where a 50% contrast $4f$ carrier plaid is modulated at frequency f (CM), a simple luminance modulation of frequency $4f$ (Carrier), luminance modulation at frequency f in which fixed 50% contrast 2-d noise is added (LM noise), and contrast modulation of 50% contrast 2-d noise at frequency f (CM noise).

Results for the 3 spatial scales are similar though they extend over different ranges of eccentricities (note scaled abscissas). The luminance stimulus (L—green diamonds) shows the characteristic monotonic falloff with eccentricity, except at the largest scale, where foveal sensitivity was less than that of the parafovea for both subjects, as found by Kehrer and Meinecke (2006; see also Pointer & Hess, 1989).

The addition of a fixed contrast $4f$ plaid component (LM—red squares) did not alter the rate of falloff with

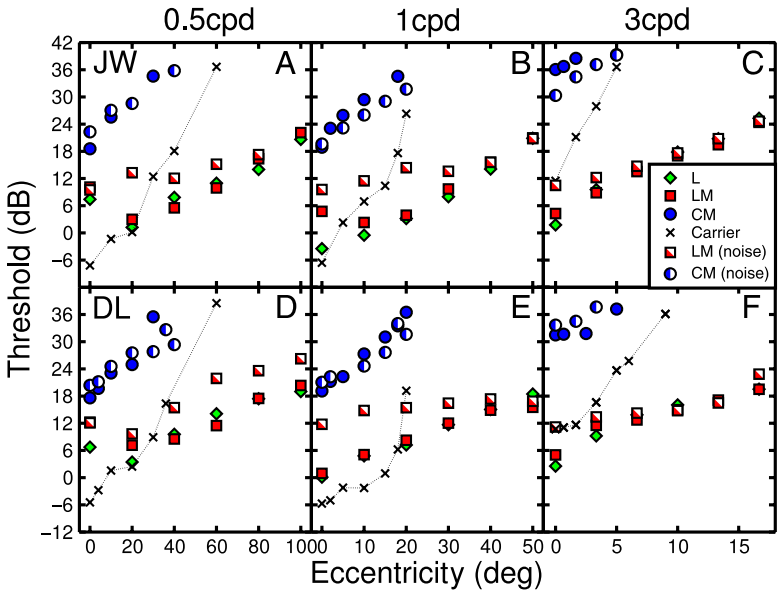

Figure 2. Results of Part I. Upper panels show data for subject JW at three spatial frequencies (viewing distances). Lower panels contain results for subject DL. Symbols denote three modulation types (L, LM, and CM), as described in the text. Half filled symbols indicate a binary noise carrier, filled symbols are for a plaid carrier at four times the modulation frequency. Performance at the carrier frequency was also measured (crosses). For clarity, error bars are not shown. The mean bootstrapped confidence interval (95th percentile minus 5th percentile) was reasonable (4.34 dB). Although the results appear similar at all spatial scales, note the change in abscissa scaling with spatial frequency.

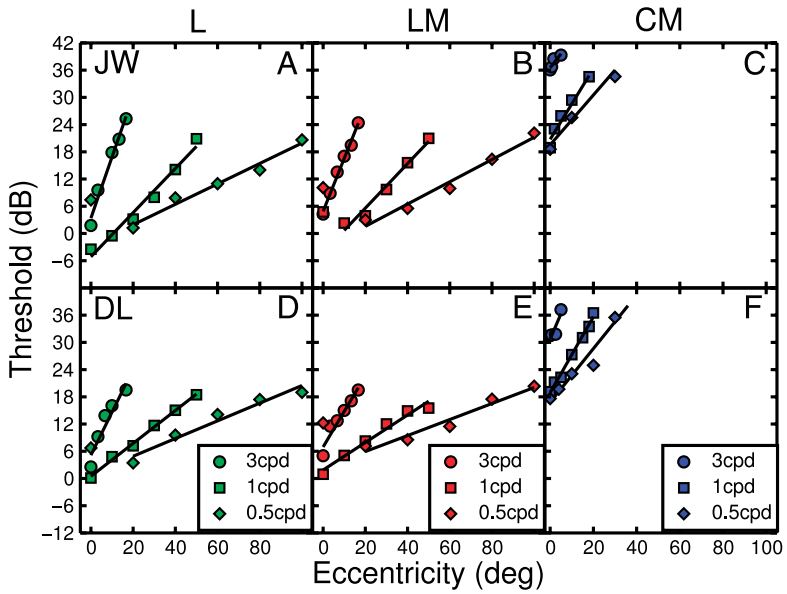

Figure 3. Threshold change with eccentricity for three spatial frequencies. Data are replotted from Figure 2 for the L (left), LM (middle), and CM (right) conditions. Lines are best fitting regression lines through the data. For the 0.5 cpd data, the foveal (0°) point was omitted from the regression for the reasons outlined in the text (L and LM conditions only).

eccentricity, although it was made considerably shallower by the addition of fixed contrast 2-d noise (LM(noise)—half-filled red squares) as a consequence of elevated central/paracentral thresholds. The CM stimulus (blue circles) exhibited a falloff with eccentricity that was comparable to that of the L (green diamonds) or LM (red squares) stimuli at the finest spatial scale (3 cpd) but was slightly steeper at the coarsest spatial scale (0.5 cpd).

In Figure 3, we replot the data for the L, LM, and CM stimuli for the three spatial frequencies on a common eccentricity scale. It is clear that the rate of the falloff with eccentricity depends both on the spatial periodicity of the stimulus and the class of stimulus (i.e., L, LM, or CM).

It appears that depending on the spatial scale tested, the 2nd order stimuli (CM and CM(noise)) mirrored either the falloff with eccentricity exhibited by the 1st order luminance-modulated stimuli (L, LM) or that expected of the higher frequency (4*f*) plaid carrier. This is summarized in Figure 4 by plotting the slopes found from the best fitting straight line to the L, LM, CM, and carrier data of Figure 3 (for the 0.5 cpd data, we did not include the foveal data for the reasons discussed above).

Figure 4A shows the average slope value across the two subjects. The carrier data (crosses) are plotted twice; first in terms of their actual spatial frequency (black) and second in terms of the low spatial frequency component to which they were either added (LM) or multiplied (CM). For both 1st and 2nd order stimuli, it is evident that sensitivity declines with eccentricity at a rate that increases with the spatial frequency of the stimulus. In Figure 4B, we plot the same data, with the slope calculated by expressing eccentricity in terms of wavelength of the stimulus, rather than degrees of visual angle. This highlights the finding that the falloff for 2nd order stimuli is not the same as for 1st order stimuli at low spatial scales.

At low modulation frequencies, the CM stimulus has an eccentricity falloff that is similar to that expected of the carrier alone (compare brown crosses and blue circles in Figure 4A). This suggests that sensitivity to the carrier may govern 2nd order detectability at coarse spatial scales—a possibility we investigate further in the Discussion. However, at 3 cpd, the CM stimulus has an eccentricity falloff that matches a 3-cpd 1st order modulation. It therefore

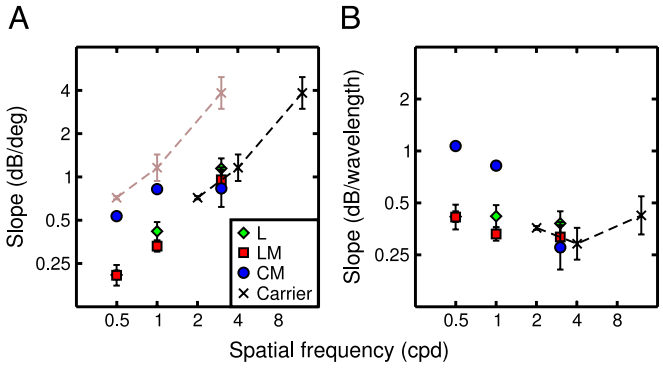

Figure 4. Change in rate of peripheral sensitivity falloff with spatial frequency. Data points are the slope values of the best fitting regression lines shown in Figure 3, averaged across two observers (geometric mean), with standard errors. Panel A shows the slope as threshold (in dB) change per degree of visual angle. The brown crosses are the carrier data transposed leftwards by a factor of 4, to aid comparison with the CM data. Panel B replots the data scaled by target wavelength.

remains possible sensitivity at finer scales is determined by other factors (see Discussion).

Part II: Equivalent noise experiments

The previously described results document two well-known differences in human visual sensitivity, namely, less sensitive peripheral detection and less sensitive CM detection. Here we ask why sensitivity is reduced in these two cases (i.e., for L stimuli with eccentricity and for detecting foveal CM stimuli). We use an equivalent noise approach to provide answers.

Figure 5 shows a comparison between foveal and peripheral (20°) results for 5 subjects for L stimuli (1 cpd) as a function of added 1-d fractal luminance noise. Following Pelli and Farrell (1999), we use a noisy linear amplifier model (LAM) to determine whether the threshold loss under noiseless conditions is due to an increased level of intrinsic noise (i.e., additive, referred to as N_{int}) or a loss of efficiency/sensitivity (i.e., multiplicative, referred to as B). In the former case, one would expect a difference between fovea and periphery in the equivalent noise (the external noise level where thresholds first begin to rise) and no threshold difference between fovea and periphery in the high noise condition (the functions should converge). On the other hand, if there is no difference in the equivalent noise and there remains a substantial threshold difference in the high noise condition (parallel functions), then the underlying problem is one of efficiency. To a first approximation, the differences appear to be attributable to internal noise (functions converge).

Subject	BT	CAS	DHB	JW	PCH	Average
B_1	0.78	0.63	0.78	0.70	0.91	0.74
B_2	0.93	0.86	0.71	0.92	0.74	0.72
N_{int1}	1.47	1.46	1.16	1.18	1.54	1.36
N_{int2}	3.44	5.28	2.40	3.70	4.25	3.12
RMSE (dB)	0.88	0.84	1.19	1.26	0.68	0.71
B_1	0.99	0.91	0.95	1.00	1.21	0.92
B_2	0.68	0.52	0.57	0.63	0.51	0.54
N_{int}	2.18	2.72	1.66	2.15	2.48	2.02
RMSE (dB)	1.56	1.94	1.73	2.16	1.61	1.46
$F_{(1,8)}$	5.42*	6.52*	4.18	5.29*	6.57*	6.08*
B	0.83	0.68	0.75	0.76	0.87	0.73
N_{int1}	1.57	1.64	1.09	1.30	1.46	1.36
N_{int2}	2.99	4.08	2.57	2.94	5.06	3.12
RMSE (dB)	0.95	0.98	1.21	1.37	0.76	0.72
$F_{(1,8)}$	1.10	2.23	0.24	1.26	1.57	0.01

Table 1. Parameters and RMS error for fits of the LAM to the data of F/P experiment. Values in the upper section give the results of the fits with four free parameters (all parameters free to vary). The lower sections show the results of keeping N_{int} (middle) or B (bottom) fixed across the two conditions. F scores are the result of a nested hypothesis test between each of the 3-parameter models (middle, bottom) and the 4-parameter model (top). Asterisks indicate that the additional free parameter in the 4-parameter model improved the fit significantly (at $p < 0.05$). All values are rounded to 2 decimal places.

However, this can also be assessed statistically using the nested models F-test.

The foveal and peripheral data in Figure 5 have been modeled in three ways. The solid curves show the fit when

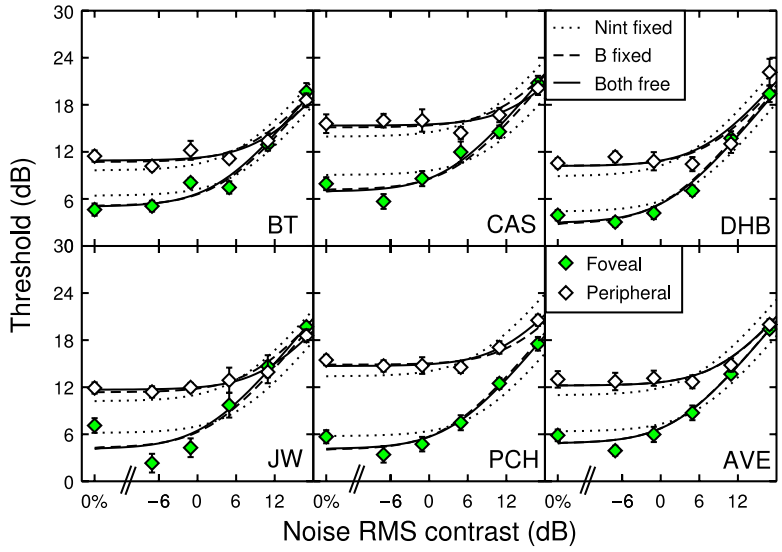

Figure 5. Noise masking functions for foveal and peripheral stimuli. Filled (green) symbols show thresholds for foveal viewing (L stimuli), open symbols are for 20° peripheral viewing. The lower right panel gives the average of all five observers. Error bars are the standard error of the probit fit for each individual subject and the standard error of the threshold estimate for the averaged data. Curves are fits of the LAM, as described in the text.

all four model parameters are free to vary (separate estimates of B and N_{int} for both the foveal and the peripheral conditions). The fit here is good for all data sets (see parameters and root mean square (RMS) errors in Table 1). The other curves are for 3-parameter versions of the model, in which one parameter remained fixed across conditions.

Inspection of Figure 5 reveals that when B is fixed (dashed lines), the fit is comparable to that of the 4-parameter model (solid lines). However, when N_{int} is fixed across conditions (dotted lines), the fit is noticeably poorer. This suggests that a difference in internal noise is responsible for the threshold differences. We confirmed this statistically using a nested hypothesis F-test, which revealed no significant difference between the 4-parameter and the 3-parameter (B fixed) models but significantly poorer fits for the 3-parameter (N_{int} fixed) model (see Table 1).

Figure 6 shows a similar analysis for foveal luminance and contrast-modulated stimuli (1 cpd) as a function of added 1-d fractal luminance noise. Using the same modeling procedure as described above, the data were fit with either 3 or 4 free parameters. The parameter values of the fits and their statistical evaluation are given in Table 2. Here, the opposite pattern is observed, with sensitivity (B) being the key parameter for 4/6 data sets. We conclude that our sensitivity for CM stimuli is reduced because of a loss of efficiency (or difference in sensitivity) of CM detectors.

Subject	BT	CAS	DHB	JW	PCH	Average
B_1	1.00	0.82	1.13	0.77	0.96	0.93
B_2	0.30	0.33	0.67	0.30	0.38	0.37
N_{int1}	1.98	1.99	1.87	1.26	1.69	1.73
N_{int2}	2.33	3.40	3.36	2.74	3.67	3.04
RMSE (dB)	1.12	1.04	0.92	1.02	0.53	0.69
B_1	1.05	0.96	1.34	0.93	1.20	1.08
B_2	0.28	0.27	0.54	0.23	0.28	0.30
N_{int}	2.12	2.55	2.43	1.75	2.42	2.24
RMSE (dB)	1.15	1.31	1.28	1.57	1.25	1.10
$F_{(1,8)}$	0.37	2.88	3.85	4.59	6.59*	4.85
B	0.86	0.73	1.02	0.70	0.89	0.83
N_{int1}	1.65	1.73	1.64	1.10	1.53	1.51
N_{int2}	8.46	8.66	5.51	7.62	9.80	7.85
RMSE (dB)	2.27	1.72	1.26	1.86	1.37	1.57
$F_{(1,8)}$	6.06*	5.03	3.73	5.57*	6.82*	6.45*

Table 2. Parameters and RMS error for fits of the LAM to the data of LM/CM experiment. The layout mirrors that of Table 1.

Discussion

The main conclusion from the first part of the study, concerning the regional variation in sensitivity of 2nd order stimuli, is that the sensitivity for detecting a contrast-modulated 2nd order stimulus declines with eccentricity, being highest at or close to the fovea. Furthermore, sensitivity declines in a spatial frequency-dependent manner; the higher the contrast-modulation frequency, the more rapid its sensitivity decline with eccentricity. Lastly, the rate of decline in sensitivity of 2nd order stimuli at fine spatial scales is similar to that of 1st order stimuli of the same spatial scale. At coarse spatial scales, the rate of decline of sensitivity with eccentricity for CM stimuli is similar to that expected from its 1st order carrier.

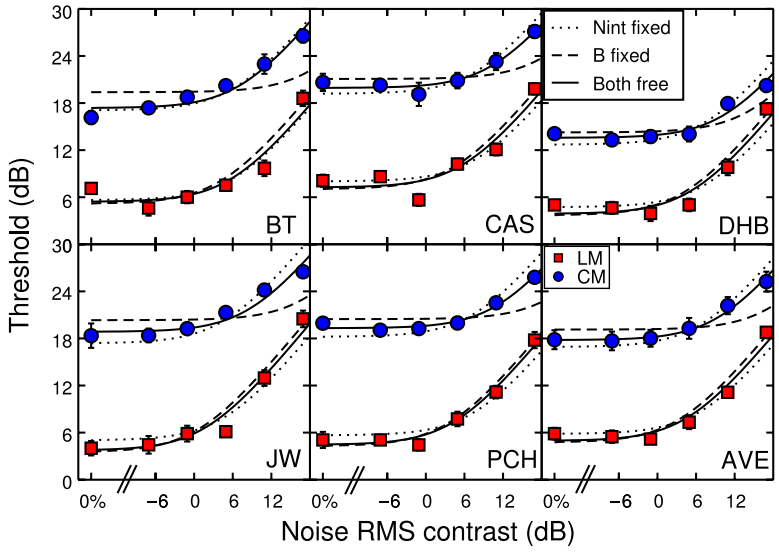

Figure 6. Noise masking functions for LM and CM stimuli, presented in the fovea. Red squares show thresholds for LM stimuli, and blue circles are thresholds for CM stimuli. The lower right panel gives the average of all five observers. Error bars are the standard error of the probit fit for each individual subject, and the standard error of the threshold estimate for the averaged data. Curves are fits of the LAM, as described in the text.

The result at fine scales is surprising. One might have intuitively expected the detection of CM stimuli always to be limited by the detection of the higher frequency carrier, given that sensitivity at this higher spatial frequency falls off much more rapidly (compare squares and crosses in Figure 2) with eccentricity (Pointer & Hess, 1989; Robson & Graham, 1981). One possibility is that there is a nonlinear relationship between carrier contrast and CM detection in the periphery. To test this, we compared CM detection for a range a carrier contrasts for foveal and peripheral loci. This explanation can be rejected because the results show that CM detection varies approximately linearly with carrier contrast for both foveal and peripheral stimuli (Figure 7).

A better explanation involves what is known about the perceived contrast of peripherally located stimuli. While it is true that more contrast is needed to detect peripherally located stimuli of any spatial scale, once the stimuli are detected, they are perceived at their veridical contrast (Georgeson & Sullivan, 1975), suggesting that the elevated peripheral thresholds are simply a consequence of a more restricted contrast range (Cannon, 1985). Thus, the perceived contrast does not vary in proportion to the threshold change. In terms of the eccentricity dependence of CM stimuli, although the degree to which the carrier is above threshold changes rapidly with eccentricity, this has no effect on CM detection until it approaches its absolute threshold. This allows the rate of falloff for CM stimuli to be primarily determined by the periodicity of their contrast modulation, as found here for fine spatial scales.

In order to test directly whether the falloff in CM sensitivity depends primarily on the frequency of the carrier or of the modulation, we ran an additional control experiment. Thresholds were gathered under the same conditions as previously, for modulation frequencies of 0.5 and 1 cpd, using an 8*f* carrier (at 3 cpd, modulations were not sufficiently detectable with this carrier to measure a reliable slope estimate). If carrier frequency is unimportant, then the slope should be constant across the

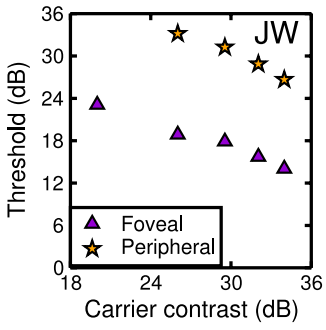

Figure 7. Effect of carrier contrast on detection of CM stimuli. Triangles are thresholds for foveal viewing, and stars are for 10° peripheral presentation. Viewing distance was 57 cm, so the spatial frequency of the modulation was 1 cpd.

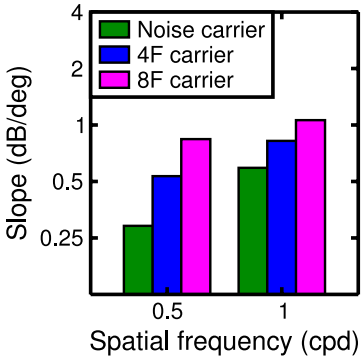

Figure 8. Change in rate of peripheral sensitivity falloff for CM stimuli with different carrier types. The 4*f* data are replotted from Figure 4, with data from the other conditions calculated using the same method and averaged across two observers.

4*f* and the 8*f* carriers. However, if carrier frequency does play a role, then the slope should change across carriers.

The results are shown in Figure 8, with the CM(noise) slopes and 4*f* carrier slopes plotted for comparison. It is clear that there is a systematic increase in slope across the different carriers, with the noise carrier yielding the shallowest slope, and the 8*f* carrier the steepest. Since the noise carrier contains frequencies below 4*f*, we assume that these govern performance in this condition. Thus, it appears that carrier properties determine detection of peripheral second order stimuli at coarse modulation scales.

In the second part of the study, we sought a better explanation, using an equivalent noise model, for why

1. the sensitivity of 1st order stimuli falls off with eccentricity; and
2. the sensitivity of foveal 2nd order stimuli is reduced compared with its 1st order counterpart.

The results suggest that the reduced sensitivity for peripheral 1st order stimuli is due to an elevated level of internal noise, and not to sampling efficiency, and that the reduced sensitivity for foveal CM stimuli is due to reduced sampling efficiency. In the following section, we seek to provide a more physiological interpretation for these two model parameters in terms of what is currently known of the contrast gain control of visual neurons.

During the course of this work, we became aware that the equivalent noise paradigm has recently been used elsewhere to characterize the threshold difference for LM and CM stimuli. One study, which used Gaussian noise, reached similar conclusions to ours (Manahilov, Simpson, & Calvert, 2005). However, a further study, which used low-pass filtered 2-d noise, concluded that CM detectors had a higher internal noise level (Allard & Faubert, 2006a). These authors used either LM or CM noise applied to the carrier in order to affect the signal within the appropriate pathway. They have recently shown (Allard & Faubert, 2006b) a double dissociation between

LM and CM stimuli in LM and CM noise (i.e., LM noise masks LM stimuli, but not CM stimuli, and vice versa). Clearly, there are important differences between their approach and ours, which uses luminance noise in all conditions, but still finds substantial masking for CM stimuli (~6 dB (a factor of 2) for some observers). Such differences highlight a shortcoming of the equivalent noise approach, as its conclusions depend on the characteristics of the stimuli used. In the following section, we reinterpret our findings in terms of contrast gain control.

Contrast gain control

As Watson et al. (1997) point out, visual masking has traditionally been considered from two perspectives. Masking using visual noise is assumed to arise because the noise increases the variance at the decision variable (output stage) of the detection process (Pelli, 1981; Pelli & Farrell, 1999). Thus, the masking is late acting and within channel. Masking using narrowband gratings, on the other hand, has been interpreted in terms of a contrast gain control (Heeger, 1992) in which populations of neurons tuned to different spatial characteristics inhibit each other. Here, masking occurs between channels, perhaps at a much earlier stage, or stages (Baker, Meese, & Summers, 2007; Freeman, Durand, Kiper, & Carandini, 2002). The gain control approach has been used extensively in grating detection (Foley, 1994), image processing (Rohaly, Ahumada, & Watson, 1997), and neural coding (Chirimuuta & Tolhurst, 2005) paradigms.

Since grating stimuli which are distant in the Fourier domain are not believed to activate common detecting mechanisms, the noise paradigm cannot accommodate cross-channel masking data, as a distant grating mask will not affect the decision variable. However, noise masks and grating masks can both be incorporated into the gain control framework. Narrowband gratings strongly activate a single inhibitory mechanism, whereas noise masks activate many mechanisms, each more weakly, causing suppression after a linear pooling process (Holmes & Meese, 2004).

The two main effects described by the LAM can be easily accommodated by a widely used gain control equation (Foley, 1994),

$$\text{resp} = \frac{C^p}{Z^q + C^q + w.M^q}, \quad (3)$$

in which C is the input (signal) contrast, M is the mask contrast (be it noise or a grating), Z is a saturation constant, w is a weight determining the impact of the mask, and p and q determine the properties of the nonlinear transducer function. Detection threshold is reached when the increase in model response caused by adding the test exceeds a criterion value, given by an additional parameter k. Although the model has several parameters (p, q, Z, w, and k), in practice some of these can be fixed at commonly used values. Here, we constrain the exponents to values used by Legge and Foley (1980), who first proposed a model of this form ($p = 2.4$, $q = 2$).

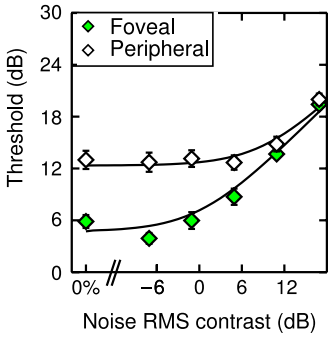

Figure 9. Gain control model fit to the average data from Part II. Data points are replotted from the lower right hand panel of Figure 5. The lower curve is the best fit of the gain control model with 3 parameters free (Z, w, and k). The upper curve was predicted by refitting one parameter (Z), while keeping the others constant. The fit is comparable to that of the LAM.

With 3 free parameters (Z, w, and k), the model provides a good fit to the foveal data (Figure 9). Increasing Z results in an increase in detection threshold and converging masking functions, as seen for the peripheral data. This is the same behavior caused by an increase in N_{int} in the LAM. However, rather than attributing this change to internal noise (as the LAM does), Z is most likely a physiological property of the detecting neurons (Z corresponds loosely to the semisaturation constant in the Naka–Rushton equation (Naka & Rushton, 1966), much favored by single cell physiologists).

Decreasing the sensitivity parameter (B) in the LAM raises thresholds and produces parallel, not convergent, masking functions. Interestingly, a comparable effect can also be achieved in the gain control model by varying the threshold criterion, k. It is noteworthy that k is thought to be proportional to the variance of late additive (internal) noise in the gain control model, yet produces very different behavior from the internal noise parameter (N_{int}) in the LAM.

Finally, by varying w, the masking function can be shifted laterally on the contrast axis. This corresponds roughly to a "mismatched perceptual template" in more elaborate forms of the LAM (Huang, Tao, Zhou, & Lu, 2007; Lu & Dosher, 1999).

It is clear that models of the gain control form are well able to describe noise masking data. Furthermore, they offer a more accurate representation of the contrast transducer that produces the familiar within-channel dipper function for contrast discrimination (Legge & Foley, 1980). Dipper functions are shifted upwards and

to the right by cross-channel grating masks (Foley, 1994), and the same behavior has also been shown using broadband noise masks (Henning & Wichmann, 2007; Pelli, 1981, 1985). The gain control model accommodates both of these findings.

The main practical use of the equivalent noise approach, and models derived from it, has been to ascribe a difference in thresholds to either a difference in sensitivity, or a difference in internal noise. From this analysis, we have concluded that the difference in thresholds with peripheral viewing is due to a change in internal noise level. However, in the gain control model, we can produce similar behavior by changing the value of *Z*. As this is merely a model parameter, can it be said to have any useful meaning?

The answer is yes. Let us assume that the value of *Z* increases with eccentricity. This will produce an increase in thresholds, as seen in Part I (Figure 2). However, due to the compressive nature of the nonlinearity at high contrasts, there will be little change in output with eccentricity at suprathreshold levels, as shown by the model response functions in Figure 10A at low and high input contrasts (dashed line vs. solid line at the starred location).

This reflects an empirically well-established phenomenon known as contrast constancy, which occurs over changes in both spatial frequency and eccentricity (Cannon, 1985; Georgeson & Sullivan, 1975). The gain control model can thus describe both the increase in detection threshold and the fidelity of high contrast stimuli at different eccentricities or spatial frequencies by varying a single parameter, *Z* (for spatial frequency, this most likely only applies to lower frequencies, where attenuation from optical factors is unimportant, i.e., below 10 cpd, Williams, Brainard, McMahon, & Navarro, 1994).

Figure 10B demonstrates this property of the model, which was originally described by Cannon and Fullenkamp (1991). The CSF was determined by estimating values of *Z* that produce detection thresholds at a range of spatial frequencies (based on the data of MAG from Georgeson & Sullivan, 1975). We then used the model to generate responses at 7 contrast levels for a single *Z* value and calculated the matching contrasts at each spatial frequency (estimated *Z* value) that produced the same magnitude of response. This produced the familiar flattening of matching functions at high contrasts, observed for both spatial frequency and peripheral viewing (Cannon, 1985).

This account also gives some insight into the behavior of 2nd order mechanisms. If the output of 1st order mechanisms, which is governed by Equation 3, forms the input to 2nd order mechanisms, then performance should be largely unaffected by changes in the detectability of the carrier at low contrasts, once it is above threshold and in the compressive region of the transducer response curve (the star in Figure 10A). Thus, second order sensitivity could be determined by constraints other than that of absolute sensitivity to the carrier, as we have found here empirically at fine spatial scales.

Conclusions

We have shown that sensitivity for 1st and 2nd order stimuli show a similar spatial frequency-dependent falloff with eccentricity. For CM detection at coarse spatial scales, the slope of this falloff is that expected of its 1st order carrier. For CM detection at fine spatial scales, the slope of the falloff is that expected of a 1st order stimulus

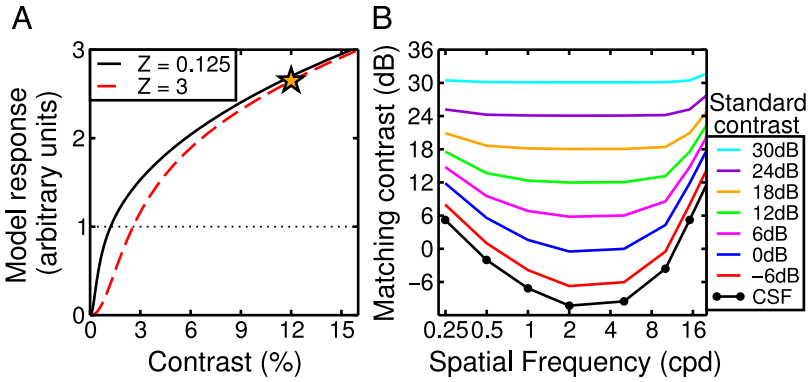

Figure 10. Model response curves and contrast matching predictions for different values of *Z*. In A, the model response is shown for a range of input contrasts. At low inputs, *Z* greatly affects the model output, leading to different thresholds (input contrasts which produce a fixed output, i.e., 1 unit (dotted line)). At higher inputs, *Z* has little effect on model response (star). In B, we show model predictions for contrast matching. The CSF is defined only by variations in *Z*, and matching performance is estimated at a range of standard contrasts, following the work of Georgeson and Sullivan (1975). At low standard contrasts, the matching functions follow the shape of the CSF, but flatten out at higher contrasts, as found empirically (Georgeson & Sullivan plot their data with an inverted ordinate).

of the same fundamental periodicity. Although such a falloff in sensitivity with eccentricity can be attributed to an increase in internal noise, our preferred explanation is that it is due to a change in the gain properties of the detecting mechanisms. The gain control approach provides a broader framework, which allows us to understand both performance (thresholds) and perception (matching) of stimuli at different spatial scales and positions in the visual field.

Acknowledgments

This research was supported by a grant from the Canadian Institutes of Health Research (MT108-18) to RFH. DHB is supported by a grant from the UK Engineering and Physical Sciences Research Council (GR/S74515/01).

Commercial relationships: none.
Corresponding author: Robert Hess.
Email: robert.hess@mcgill.ca.
Address: McGill Vision Research, 687 Pine Avenue, W. Rm. H4-14, Montréal, Québec, Canada H3A 1A1.

References

Allard, R., & Faubert, J. (2006a). Contrast-modulated stimuli detection is unaffected by luminance modulated noise [Abstract]. *Journal of Vision, 6*(6):378, 378a, http://journalofvision.org/6/6/378/, doi:10.1167/6.6.378.

Allard, R., & Faubert, J. (2006b). Same calculation efficiency but different internal noise for luminance- and contrast-modulated stimuli detection. *Journal of Vision, 6*(4):3, 322–334, http://journalofvision.org/6/4/3/, doi:10.1167/6.4.3. [PubMed] [Article]

Baker, C. L., Jr. (1999). Central neural mechanisms for detecting second-order motion. *Current Opinion in Neurobiology, 9,* 461–466. [PubMed]

Baker, D. H., Meese, T. S., & Summers, R. J. (2007). Psychophysical evidence for two routes to suppression before binocular summation of signals in human vision. *Neuroscience, 146,* 435–448. [PubMed]

Banks, M. S., Geisler, W. S., & Bennett, P. J. (1987). The physical limits of grating visibility. *Vision Research, 27,* 1915–24. [PubMed]

Cannon, M. W., Jr. (1985). Perceived contrast in the fovea and periphery. *Journal of the Optical Society of America A, Optics and Image Science, 2,* 1760–1768. [PubMed]

Cannon, M. W., & Fullenkamp, S. C. (1991). A transducer model for contrast perception. *Vision Research, 31,* 983–998. [PubMed]

Chirimuuta, M., & Tolhurst, D. J. (2005). Does a Bayesian model of V1 contrast coding offer a neurophysiological account of human contrast discrimination? *Vision Research, 45,* 2943–2959. [PubMed]

Cornsweet, T. N. (1962). The staircase-method in psychophysics. *American Journal of Psychology, 75,* 485–491. [PubMed]

Daniel, P. M., & Whitteridge, D. (1961). The representation of the visual field on the cerebral cortex in monkeys. *The Journal of Physiology, 159,* 203–221. [PubMed] [Article]

Ellemberg, D., Allen, H. A., & Hess, R. F. (2006). Second-order spatial frequency and orientation channels in human vision. *Vision Research, 46,* 2798–2803. [PubMed]

Finney, D. (1971). *Probit analysis*. Cambridge: Cambridge University Press.

Foley, J. M. (1994). Human luminance pattern-vision mechanisms: Masking experiments require a new model. *Journal of the Optical Society of America A, Optics, Image Science, and Vision, 11,* 1710–1719. [PubMed]

Freeman, T. C., Durand, S., Kiper, D. C., & Carandini, M. (2002). Suppression without inhibition in visual cortex. *Neuron, 35,* 759–771. [PubMed] [Article]

Georgeson, M. A., & Sullivan, G. D. (1975). Contrast constancy: Deblurring in human vision by spatial frequency channels. *The Journal Physiology, 252,* 627–56. [PubMed] [Article]

Heeger, D. J. (1992). Normalization of cell responses in cat striate cortex. *Visual Neuroscience, 9,* 181–197. [PubMed]

Henning, G. B., & Wichmann, F. A. (2007). Some observations on the pedestal effect. *Journal of Vision, 7*(1):3, 1–15, http://journalofvision.org/7/1/3/, doi:10.1167/7.1.3. [PubMed] [Article]

Holmes, D. J., & Meese, T. S. (2004). Grating and plaid masks indicate linear summation in a contrast gain pool. *Journal of Vision, 4*(12):7, 1080–1189, http://journalofvision.org/4/12/7/, doi:10.1167/4.12.7. [PubMed] [Article]

Huang, C., Tao, L., Zhou, Y., & Lu, Z. (2007). Treated amblyopes remain deficient in spatial vision: A contrast sensitivity and external noise study. *Vision Research, 47,* 22–34. [PubMed]

Hubel, D. H., & Wiesel, T. N. (1977). Ferrier lecture. Functional architecture of macaque monkey visual cortex. *Proceedings of the Royal Society of London B: Biological Sciences, 198,* 1–59. [PubMed]

Hutchinson, C. V., & Ledgeway, T. (2006). Sensitivity to spatial and temporal modulations of first-order and second-order motion. *Vision Research, 46,* 324–35. [PubMed]

Johnson, A. P., & Baker, C. L., Jr. (2004). First- and second-order information in natural images: A filter-based approach to image statistics. *Journal of the Optical Society of America A, Optics, Image Science, and Vision, 21,* 913–925. [PubMed]

Kehrer, L., & Meinecke, C. (2006). A 'first stage' central performance drop in a Gabor luminance-modulation detection task. *Spatial Vision, 19,* 427–437. [PubMed]

Legge, G. E., & Foley, J. M. (1980). Contrast masking in human vision. *Journal of the Optical Society of America, 70,* 1458–1471. [PubMed]

Lu, Z. L., & Dosher, B. A. (1999). Characterizing human perceptual inefficiencies with equivalent internal noise. *Journal of the Optical Society of America A, Optics, Image Science, and Vision, 16,* 764–778. [PubMed]

Manahilov, V., Simpson, W. A., & Calvert, J. (2005). Why is second-order vision less efficient than first-order vision? *Vision Research, 45,* 2759–2772. [PubMed]

Naka, K. I., & Rushton, W. A. (1966). S-potentials from luminosity units in the retina of fish (Cyprinidae). *The Journal of Physiology, 185,* 587–599. [PubMed] [Article]

Nelder, J. A., & Mead, R. (1965). A simplex method for function minimization. *Computer Journal, 7,* 308–313.

Peichl, L., & Wassle, H. (1979). Size, scatter and coverage of ganglion cell receptive field centres in the cat retina. *The Journal of Physiology, 291,* 117–141. [PubMed] [Article]

Pelli, D. G. (1990). The quantum efficiency of vision. In C. Blakemore (Ed.), *Vision coding and efficiency* (pp. 3–24). Cambridge: Cambridge University Press.

Pelli, D. G. (1981). *The effects of visual noise*. PhD thesis, Cambridge University, Cambridge, UK.

Pelli, D. G. (1985). Uncertainty explains many aspects of visual contrast detection and discrimination. *Journal of the Optical Society of America A, Optics and Image Science, 2,* 1508–1532. [PubMed]

Pelli, D. G., & Farell, B. (1999). Why use noise? *Journal of the Optical Society of America A, Optics, Image Science, and Vision, 16,* 647–653. [PubMed]

Pointer, J. S., & Hess, R. F. (1989). The contrast sensitivity gradient across the human visual field: With emphasis on the low spatial frequency range. *Vision Research, 29,* 1133–1151. [PubMed]

Robson, J. G., & Graham, N. (1981). Probability summation and regional variation in contrast sensitivity across the visual field. *Vision Research, 21,* 409–418. [PubMed]

Rodieck, R. W. (1973). *The vertebrate retina*. San Francisco: W. H. Freeman.

Rohaly, A. M., Ahumada, A. J., Jr., & Watson, A. B. (1997). Object detection in natural backgrounds predicted by discrimination performance and models. 3225–3235. [PubMed]

Sutter, A., Sperling, G., & Chubb, C. (1995). Measuring the spatial frequency selectivity of second-order texture mechanisms. *Vision Research, 35,* 915–924. [PubMed]

Van Nes, F. L., & Bouman, M. A. (1967). Spatial modulation transfer in the human eye. *Journal of the Optical Society of America A, 57,* 401–406.

Watson, A. B., Borthwick, R., & Taylor, M. (1997). Image quality and entropy masking. *SPIE Proceedings, 3016,* 1–11.

Wertheim, T. (1894). Uber die indirekte Sehschärfe. *Zeitschrift fur Psychologie, 7,* 172–189.

Wetherill, G. B., & Levitt, H. (1965). Sequential estimation of points on a psychometric function. *British Journal of Mathematical and Statistical Psychology, 18,* 1–10. [PubMed]

Williams, D. R., Brainard, D. H., McMahon, M. J., & Navarro, R. (1994). Double-pass and interferometric measures of the optical quality of the eye. *Journal of the Optical Society of America A, Optics, Image Science, and Vision, 11,* 3123–3135. [PubMed]

Zhou, Y. X., & Baker, C. L., Jr. (1993). A processing stream in mammalian visual cortex neurons for non-Fourier responses. *Science, 261,* 98–101. [PubMed]